ISSN 1070-3284, Russian Journal of Coordination Chemistry, 2014, Vol. 40, No. 5, pp. 314–319. © Pleiades Publishing, Ltd., 2014.

A Novel Lanthanide-Organic Wave-Like Network with 1*H*-Imidazole-4,5-Dicarboxylate and Oxalate: Structure, Photoluminescence, and Magnetic Properties[1]

L. Liu[a, b], J. Liu[a], X. Feng[b, *], S. Yang[b], and L. Y. Wang[b, c, **]

[a] *College of Chemistry and Molecular Engineering, Zhengzhou University, Zhengzhou, 450001 P.R. China*

[b] *College of Chemistry and Chemical Engineering, Luoyang Normal University, Luoyang, 471022 P.R. China*

[c] *College of Chemistry and Pharmacy Engineering, Nanyang Normal University, Nanyang, 473601 P.R. China*

*e-mail: * fengx@lynu.edu.cn; ** wlya@lynu.edu.cn*

Received August 4, 2013

Abstract—The solvothermal reaction of lanthanide nitrate and H_4Diida ligand (H_4Diida = 2-(4,5-dicarboxy-1*H*-imidazol-2-yl)-1*H*-imidazole-4,5-dicarboxylic acid) in the presence of ammonium oxalate results in a new three-dimensional (3D) lanthanide-organic framework, namely, $\{[Pr(Ida)(\mu_2\text{-}C_2O_4)_{0.5}(H_2O)_2] \cdot H_2O\}_n$ (H_2Ida = 1*H*-imidazole-4,5-dicarboxylic acid). H_4Diida ligand can be in situ into Ida^{2-} ions under the conditions, as unequivocally proved by these similar situations occurred in other systems. Single crystal X-ray diffraction analysis reveals the formation of a novel wave-like structure. It crystallizes in the monoclinic system, space group of $P2_1/c$. The polymer is built from two kinds of parallel alternately 1D infinite chain through the carboxylate double-linking adjacent Pr^{3+} cations, forming an extended 2D bilayer-like structure along the *yz* plane. Moreover, the polymer further stacks via weak interactions to generate a 3D supramolecular framework. The photoluminescence and magnetic properties for the polymer were also investigated and discussed.

DOI: 10.1134/S1070328414040058

INTRODUCTION

Nowadays, as an important branch in the field of crystal engineering, the reasonable design and preparation of lanthanide-organic frameworks (LnOFs) have become an attractive research field, mainly owing to their compositional and structural diversities, as well as potential applications in catalysis, ion exchange, magnetism, intercalation chemistry, photochemistry and materials chemistry [1–4]. Meanwhile, the imidazole and its derivatives are widely employed as functional ligands in coordination chemistry. The imidazole ring tends to adopt bidentate/bridging/tridentate for imidazolate anions to construct polynuclear or extending structures [5, 6]. In this paper, H_4Diida (H_4Diida = 2-(4,5-dicarboxy-1*H*-imidazol-2-yl)-1*H*-imidazole-4,5-dicarboxylic acid), a multifunctional ligand which has six sites for potential coordination to a metal center which contribute to increase the dimensionality of the assembled networks, has attracted much interest [7, 8]. Intriguingly, a new lanthanide-organic polymer $\{[Pr(Ida)(\mu_2\text{-}C_2O_4)_{0.5}(H_2O)_2] \cdot H_2O\}_n$ (**I**) (H_2Ida = 1*H*-imidazole-4,5-dicarboxylic acid) was obtained by the solvothermal reaction of lanthanide nitrate, ammonium oxalate and H_4Diida ligand. With no Ida^{2-} ligand directly introduced to the starting materials, we supposed that Ida^{2-} ligand might be derived from the decomposition of H_4Diida, similar situations also occurred in other systems [9, 10]. The synthesis, crystal structure, and thermal stability as well as the solid-state luminescence property of the polymer **I** are reported herein.

EXPERIMENTAL

Materials and physical measurements. All reagents used in the syntheses were of analytical grade and used as received. The infrared spectra (4000–400 cm^{-1}) were recorded by using KBr pellet on an Avatar™ 360 ESP IR spectrometer. Thermogravimetry-differential thermal analysis was recorded using a SDT 2960 simultaneous thermal analyzer (DTA Instruments, New Castle, DE) in N_2 atmosphere at a heating rate of 10°C min^{-1} from 30 to 900°C. Solid luminescence spectrum of the polymer was run on a Cary Eclipse fluorescence spectrophotometer. Variable-temperature magnetic susceptibilities were measured using a MPMS-7 SQUID magnetometer under a 0.2 T applied magnetic field and over the range of 2 to 300 K. Diamagnetic corrections were made with Pascal's constants for all constituent atoms.

Synthesis of $\{[Pr(Ida)(\mu_2\text{-}C_2O_4)_{0.5}(H_2O)_2] \cdot H_2O\}_n$. 2-(4,5-Dicarboxy-1*H*-imidazol-2-yl)-1*H*-imidazole-4,5-dicarboxylic acid (0.032 g, 0.1 mmol) and ammonium oxalate (0.015 g, 0.1 mmol) in a solution of wa-

[1] The article is published in the original.

ter–alcohol (v : v = 1.2, 10 mL) were mixed with an aqueous solution (10 mL) of $Pr(NO_3)_3 \cdot 6H_2O$ (0.043 g, 0.1 mmol). After stirring for 20 min in air, the pH value was adjusted to 3.5 with nitric acid, and the mixture was placed into 25 mL Teflon-lined autoclave under autogenous pressure being heated at 155°C for 72 h, then the autoclave was cooled over a period of 24 h at a rate 5°C/h. After filtration, the product was washed with distilled water and then dried, yellow crystal of polymer **I** was obtained suitable for X-ray diffraction analysis.

X-ray crystallography. Single-crystal diffraction data of polymer **I** was collected on a Bruker SMART APEX CCD diffractometer with graphite-monochromated MoK_α radiation (λ = 0.71073 Å) at room temperature. The structure was solved using direct methods and successive Fourier difference synthesis (SHELXS-97) [11] and refined using the full-matrix least-squares method on F^2 with anisotropic thermal parameters for all nonhydrogen atoms (SHELXL-97) [12]. The disordered ethyl carbon atoms of Ida^{2-} ligand were restrained in order to obtain reasonable thermal parameters. The hydrogen atoms of organic ligands were placed in calculated positions and refined using a riding on attached atoms with isotropic thermal parameters 1.2 times those of their carrier atoms. The summary crystallographic data for polymer **I** are given in Table 1, selected bond lengths and angles are listed in Table 2.

Crystallographic data for the structure **I** have been deposited with the Cambridge Crystallographic Data Centre (no. 940831; http://www.ccdc.cam.ac.uk/conts/retrieving.html).

RESULTS AND DISCUSSION

Single crystal X-ray diffraction analysis reveals that polymer **I** crystallizes in the monoclinic system with space group of $P2_1/c$. As illustrated in Fig. 1, the asymmetric unit of **I** contains one lanthanide center Pr(1), one N(1) atom belonging to Ida^{2-} ligand and eight O-atoms, among which two O(1), O(2) atoms are from oxalate ligand, four O(3), O(4), O(5), O(6) atoms are from carboxylate of three symmetry-related Ida^{2-} ligands and two O(7), O(8) atoms are coordination water oxygen atoms. This leads to a nine-coordination sphere, which resembles a highly distorted tricapped trigonal geometry with Pr–O bond lengths ranging from 2.425(3) to 2.632(2) Å, and the Pr–N bond distance being 2.608(3) Å. Additionally, the distortion of lanthanide coordination sphere is clearly reflected by the internal (N,O)–Pr–O bond angles: while the OPrO angles range between 63.79(8)° and 141.45(10)°, and the NPrO angles have been found to be in the range of 62.62(8)° to 142.45(9)°.

The coordination environment of Ida^{2-} (a) and oxalate (b) in polymer **I** is illustrated below:

Table 1. Crystallographic data and experimental details for polymer **I**

Parameter	Value
Empirical formula	$C_6H_7N_2O_9Pr$
Formula weight	392.05
Temperature	293(2)
Crystal system	Monoclinic
Space group	$P2_1/c$
a, Å	7.5071(15)
b, Å	17.255(4)
c, Å	8.5855(17)
β, deg	110.927(2)
V, Å^3	1038.8(4)
Z	4
ρ, g cm^{-3}	2.507
F(000)	752.0
Crystal size, mm^3	0.22 × 0.19 × 0.17
2θ Range for data collection, deg	4.72–56.56
Limiting indice rangs	$-9 \le h \le 10$, $-9 \le k \le 23$, $-11 \le l \le 11$
Reflections collected/unique	5533/2037
R_{int}	0.0610
Reflections with ($I > 2\sigma(I)$)	1979
Max. and min. transmissions	0.4997, 0.4221
Data/restraints/parameters	2508/0/168
GOOF	1.119
R_1, wR_2 ($I > 2\sigma(I)$)	0.0249, 0.0626
R_1, wR_2 (all data)	0.0260, 0.0632
Largest diff. peak and hole, e/Å^3	0.807 and –1.168

$R_1 = [\Sigma \|F_o| - |F_c\|/\Sigma|F_o|]$, $wR_2 = \Sigma_{Ww}[|F_o^2 - F_c^2|^2/\Sigma_W(|F_w|^2)^2]^{1/2}$.

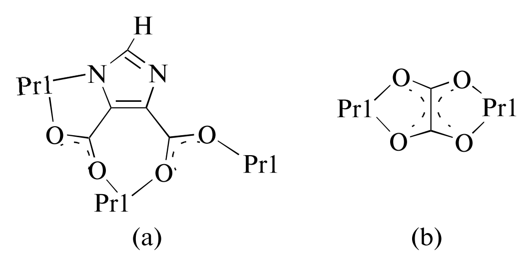

Scheme.

The oxalate ion is structurally located at a symmetry plane and bridges two symmetry-related lanthanide cations via a bis-bidentate chelate interaction, act as a tetradentate ligand [13]. These O,O-chelate interactions are crystallographic equivalent with a chelating angle of 63.79(8)° and originate an intermetallic Pr(1)···Pr(1) distance of 6.5427(8) Å. The Ida^{2-} anionic ligand connects three crystallographically

Table 2. Selected bond lengths (Å) and bond angles (deg) for polymer **I***

Bond	*d*, Å	Bond	*d*, Å	Bond	*d*, Å
Pr(1)–O(1)$^{\#1}$	2.534(2)	Pr(1)–O(3)	2.425(3)	Pr(1)–O(2)	2.540(2)
Pr(1)–O(4)$^{\#2}$	2.632(2)	Pr(1)–O(7)	2.565(3)	Pr(1)–O(5)	2.452(2)
Pr(1)–O(6)$^{\#3}$	2.537(2)	Pr(1)–O(8)	2.496(3)	Pr(1)–N(1)$^{\#3}$	2.608(3)
Angle	ω, deg	Angle	ω, deg	Angle	ω, deg
O(1)$^{\#1}$Pr(1)O(2)	63.79(8)	O(3)Pr(1)N(1)$^{\#3}$	75.04(9)	O(5)Pr(1)N(1)$^{\#3}$	75.92(9)
O(1)$^{\#1}$Pr(1)O(4)$^{\#2}$	70.75(8)	O(2)Pr(1)O(4)$^{\#2}$	70.95(8)	O(6)$^{\#3}$Pr(1)O(2)	67.12(8)
O(1)$^{\#1}$Pr(1)O(7)	124.82(8)	O(2)Pr(1)O(7)	132.89(8)	O(6)$^{\#3}$Pr(1)O(4)$^{\#2}$	129.59(7)
O(1)$^{\#1}$Pr(1)O(6)$^{\#3}$	111.94(8)	O(2)Pr(1)N(1)$^{\#3}$	88.60(9)	O(6)$^{\#3}$Pr(1)O(7)	122.93(8)
O(1)$^{\#1}$Pr(1)N(1)$^{\#3}$	72.00(9)	O(7)Pr(1)O(4)$^{\#2}$	70.64(8)	O(6)$^{\#3}$Pr(1)N(1)$^{\#3}$	62.62(8)
O(3)Pr(1)O(1)$^{\#1}$	73.38(9)	O(7)Pr(1)N(1)$^{\#3}$	138.28(9)	O(8)Pr(1)O(1)$^{\#1}$	134.61(9)
O(3)Pr(1)O(2)	137.06(8)	O(5)Pr(1)O(1)$^{\#1}$	139.92(8)	O(8)Pr(1)O(2)	77.61(8)
O(3)Pr(1)O(4)$^{\#2}$	98.49(8)	O(5)Pr(1)O(2)	138.88(8)	O(8)Pr(1)O(4)$^{\#2}$	74.89(8)
O(3)Pr(1)O(7)	75.05(9)	O(5)Pr(1)O(4)$^{\#2}$	139.31(8)	O(8)Pr(1)O(7)	66.87(9)
O(3)Pr(1)O(5)	75.65(8)	O(5)Pr(1)O(7)	68.96(9)	O(8)Pr(1)O(6)$^{\#3}$	69.96(8)
O(3)Pr(1)O(6)$^{\#3}$	131.36(8)	O(5)Pr(1)O(6)$^{\#3}$	71.95(8)	O(8)Pr(1)N(1)$^{\#3}$	132.28(8)
O(3)Pr(1)O(8)	141.45(10)	O(5)Pr(1)O(8)	85.13(8)	N(1)$^{\#3}$Pr(1)O(4)$^{\#2}$	142.45(9)

* Symmetry codes: $^{\#1}$ $-x, 1-y, 2-z$; $^{\#2}$ $-x, 1-y, 1-z$; $^{\#3}$ $x, 3/2-y, 1/2+z$; $^{\#4}$ $x, 3/2-y, -1/2+z$.

equivalent Pr(III) centers via three distinct coordination modes (see scheme), ultimately occurring in the crystal structure as a pentadentate ligand. On the one hand, the heteroatoms of the aromatic ring form along, with the adjacent carboxylate groups, two equivalent N,O-chelate interactions with the observed chelating angles being of 62.616(5)°. On the other hand, two O-atoms of two carboxylate groups, coordinate via a bidentate interaction with the OPrO angle being of 75.648(6)° [14, 15].

Further investigation of the crystal structure of polymer **I** reveals that the Pr^{3+} cations are connected to each other with Pr···Pr separation of 7.0263(10) Å through the bridging Ida^{2-} ligands, leading to a 1D in-

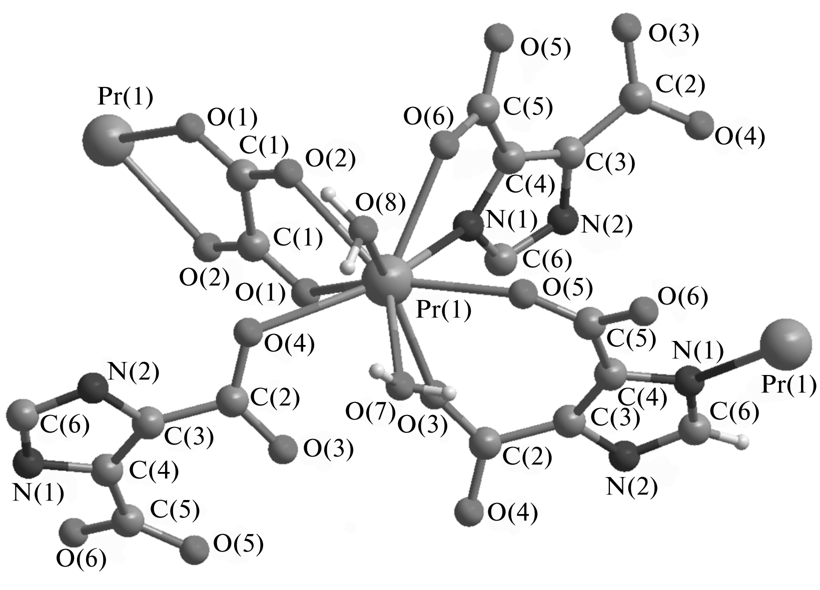

Fig. 1. The coordination environments of Pr^{3+} ions in **I**. Free water molecules have been omitted for clarity.

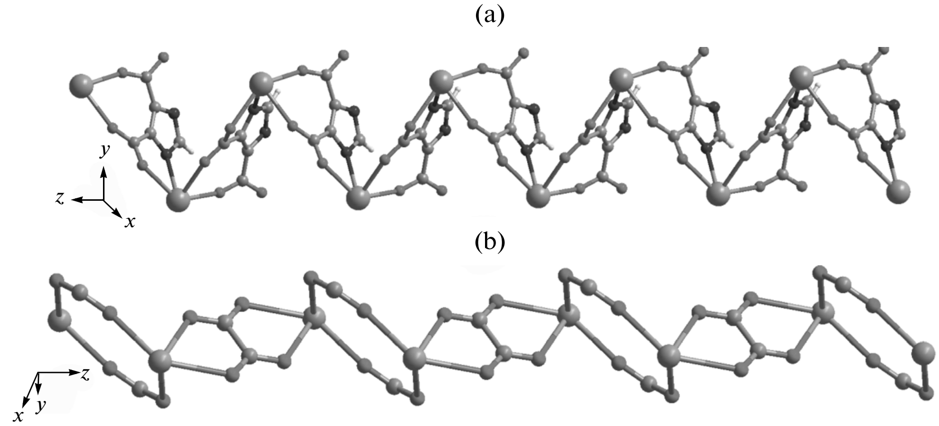

Fig. 2. 1D zigzag chain of $[Pr(Ida)]_n$ linked by the Ida^{2-} ligands viewed along *x* axis in polymer **I** (a); 1D ladder-like chain of Pr^{3+} cations linked by the oxalate ligands and carboxylate oxygen atoms in polymer **I** (b).

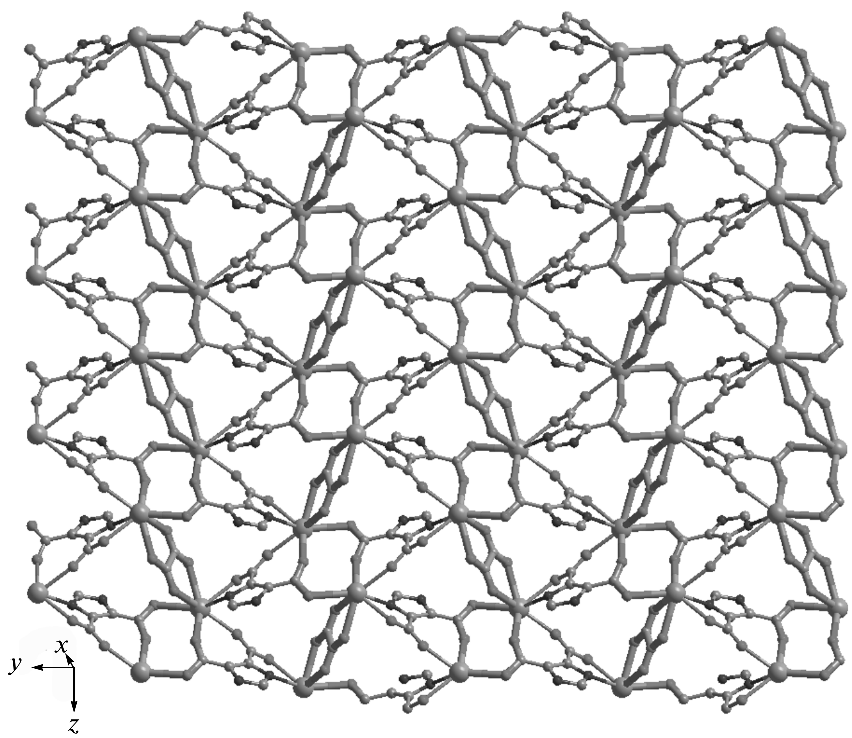

Fig. 3. View of a 2D bilayer-like network in polymer **I** assembled by alternate two kinds of parallel infinite chains.

finite zigzag chain-like structure of $[Pr(Ida)]_n$ paralleling to the *z* axis (Fig. 2a) [16]. In addition, two crystallographic equivalent Pr^{3+} cations possessing a octatomic ring are bridged by two equivalent carboxylate units (O(3)–C(2)–O(4) carboxylic group belonging to two symmetry-related Ida^{2-} ligands), resulting in a binuclear $[Pr_2(CO_2)_2]$ motif with a Pr···Pr distance of 5.1142(7) Å (Fig. 2b) [17, 18]. Each oxalate anion links two $[Pr_2(CO_2)_2]$ unit with all the Pr^{3+} cations being in the different plane, forming a 1D infinite ladder-like $[Pr_2(CO_2)_2(\mu_2\text{-}C_2O_4)]_n$ chain. The adjacent $[Pr_2(CO_2)_2(\mu_2\text{-}C_2O_4)]_n$ chains are further connected by Ida^{2-} ligand, forming a 2D network along to the *yz* plane (Fig. 3), leading to a novel double-link structure. On the basis of these connection, all the Pr(III) cations are located in two different planes, exhibiting a fantastic 2D wave-like structure viewed from *z* axis (Fig. 4). Moreover these 2D wave-like bilayer units

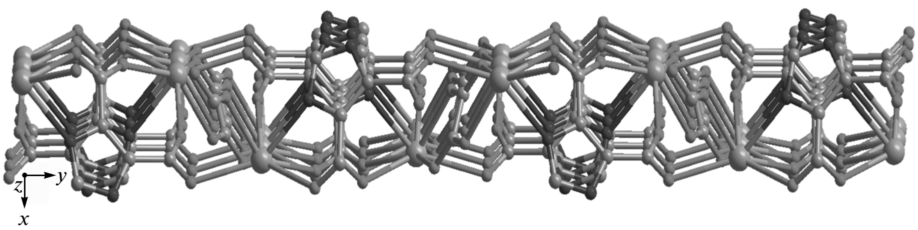

Fig. 4. View of 2D wave-like structure in polymer **I**.

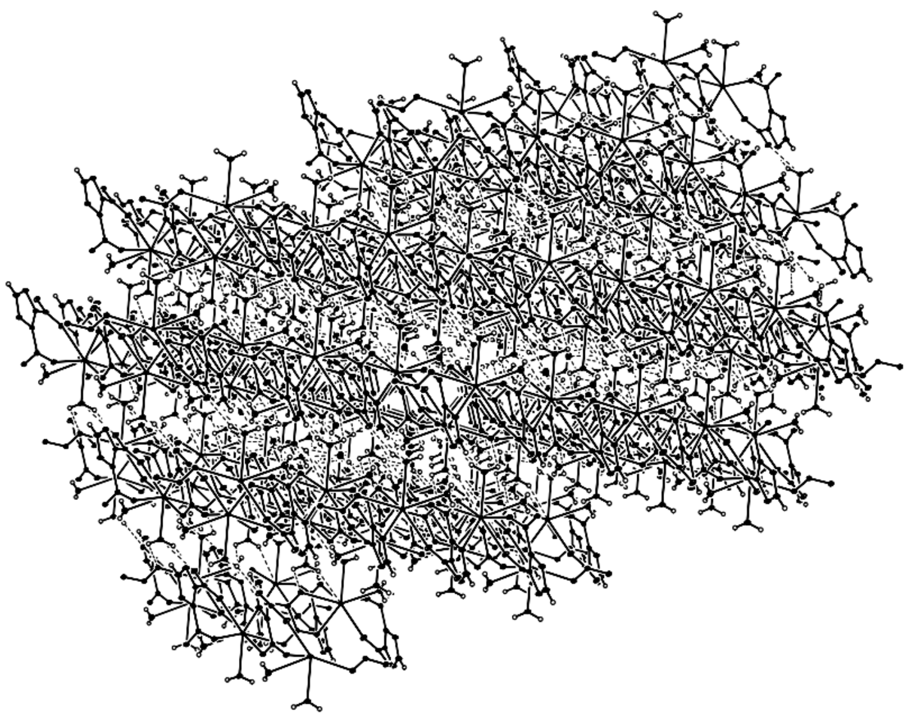

Fig. 5. 3D supra-molecular network of **I** stacks together via π···π stack packing interactions and weak hydrogen bonding.

stack together via π···π stack packing interactions and weak hydrogen bonding, resulting in formation of a 3D supramolecular network (Fig. 5) [19, 20].

In order to check the phase purity of sample **I**, the X-ray powder diffraction (XRPD) pattern was checked at room temperature. The peak positions of the simulated and experimental XRPD patterns are nearly in agreement with each other, demonstrating the good phase purity of **I**.

The thermo-gravimetry diagram of **I** exhibits an initial mass loss of 14.2% corresponding to start with the departure of the coordinated and uncoordinated water molecules (calcd. 13.7%). The network mass of **I** is stable up to ~330°C, upon further heating, a weight loss is 37.9% in the temperature range of 330–900°C, which corresponds to the destruction of the Ida^{2-} organic ligands and oxalate, consistent with the crystal structure analysis. Since the limitation of instrument, the final temperature was set at 900°C with weight percent of **I** still decreasing. The final value of 46.7% at 900°C is close to the calculated value of 43.4% based on an assuming product Pr_6O_{11} phase.

The solid photoluminescence property of the sample of **I** was investigated at room temperature upon photo-excitation with 329 nm. The photoluminescence of **I** is quite similar with other imidazole dicarboxylic acid ligand [21]. The emission spectrum of polymer **I** exhibits one broad and sharp emission with maximum wavelength of $\lambda_{max} = 372$ nm, which can be assigned to the π–π* or *n*–*n** intraligand fluorescence.

Variable-temperature magnetic susceptibility measurements were performed on microcrystalline samples of polymer **I**. The temperature dependence of the magnetic susceptibility of polymer **I** is reported in Fig. 6. The $\chi_M T$ value of **I** is 1.62 cm^3 mol^{-1} K at 300 K, which is nearly agree with the expected value for a magnetically uncoupled Pr^{3+} ion (1.60 cm^3 mol^{-1} K)

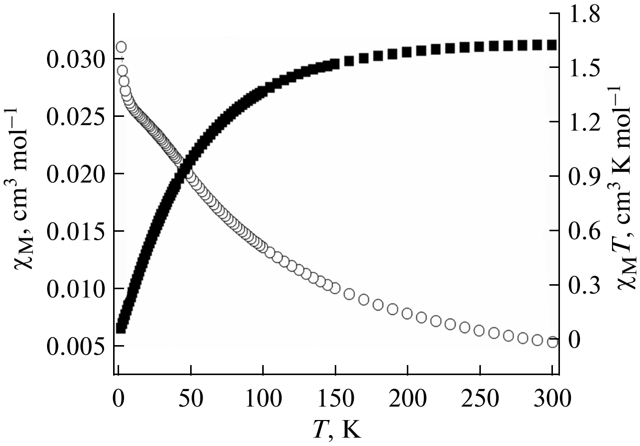

Fig. 6. Experimental magnetic data plotted as $\chi_M T$ (■) and χ_M (○) for **I** under an applied field of 0.2 T between 2 and 300 K.

in the $^3H_4$ ground state ($g = 4/5$) [22]. Upon cooling, the $\chi_M T$ decreases with the measurement temperature up to 2 K, where it arrives at the minimum value of 0.062 cm^3 mol^{-1} K. This behavior may be a consequence of the crystal field effect, which partially removes the $2J + 1$ degeneracy of the ground state $^3H_4$ in zero fields, or the possible weak antiferromagnetic interaction within polymer **I** [23].

ACKNOWLEDGMENTS

This work was supported by the National Natural Science Foundation of China (nos. 21271098 and 21273101), the Program for Backbone Teachers in Universities of Henan Province (no. 12GGJS158), and Key Problem of Science and Technology Project of Henan Province (no. 142102310483).

REFERENCES

1. Soares-Santos, P.C.R., Cunha-Silva, L., Paz, F.A.A., et al., *Inorg. Chem.*, 2010, vol. 49, no. 7, p. 3428.
2. Sun, Y.Q., Zhang, J., and Yang, G.Y., *Dalton Trans.*, 2003, no. 18, p. 3634.
3. Chen, K., Dong, D.P., Sun, Z.G., et al., *Dalton Trans.*, 2012, vol. 41, p. 10948.
4. Hong, M.C., Zhao, Y.J., Su, W.P., et al., *Angew. Chem. Int. Ed.*, 2000, vol. 39, no. 14, p. 2468.
5. Dolbecq, A., Mialane, P., Sécheresse, F., et al., *Chem. Commun.*, 2012, vol. 48, no. 67, p. 8299.
6. Zhang, L.J., Xu, S., Zhou, Y.S., et al., *CrystEngComm*, 2011, vol. 13, no. 21, p. 6511.
7. Zhu, Y.Y., Sun, Z.G., Tong, F., et al., *Dalton Trans.*, 2011, vol. 40, no. 20, p. 5584.
8. Hou, K.L., Bai, F.Y., Xing, Y.H., et al., *CrystEngComm*, 2011, vol. 13, no. 11, p. 3884.
9. Fan, J., Wang, Z.H., Yang, M., et al., *CrystEngComm*, 2010, vol. 12, no. 1, p. 216.
10. Zeng, R.R., Zhai, Q.G., and Li, S.N., *CrystEngComm*, 2011, vol. 13, no. 15, p. 4823.
11. Sheldrick, G.M., *SHELXS-97, Program for the Solution of Crystal Structure*, Göttingen (Germany): Univ. of Göttingen, 1997.
12. Sheldrick, G.M., *SHELXL-97, Program for the Crystal Structure Refinement*, Göttingen (Germany): Univ. of Göttingen, 1997.
13. Ma, C.B., Chen, F., Chen, C.N., and Liu, Q.T., *Acta Crystallogr., C*, 2003, vol. 59, p. 516.
14. Chen, L.Z., Wang, F.M., and Cao, X.X., *Chin. J. Struct. Chem.*, 2012, vol. 31, no. 10, p. 1417.
15. Du, C.J., Song, X.H., Wang, L.S., and Du, C.L., *Acta Crystallogr., E*, 2011, vol. 67, p. 997.
16. Zhang, X.J., Xing, Y.H., Han, J., et al., *Cryst. Growth Des.*, 2008, vol. 8, no. 10, p. 3680.
17. Liu, M.S., Yu, Q.Y., Cai, Y.P., et al., *Cryst. Growth Des.*, 2008, vol. 8, no. 11, p. 4083.
18. Tang, Y.Z., Wen, H.R., Cao, Z., et al., *Inorg. Chem. Commun.*, 2010, vol. 13, no. 8, p. 924.
19. Li, B., Gu, W., Zhang, L.Z., et al., *Inorg. Chem.*, 2006, vol. 45, no. 26, p. 10425.
20. Feng, X., Liu, B., Wang, L.Y., et al., *Dalton Trans.*, 2010, vol. 39, no. 34, p. 8038.
21. Cao, D.K., Zhang, Y.H., Huang, J., et al., *RSC Advances*, 2012, vol. 2, no. 16, p. 6680.
22. Xu, N., Shi, W., Liao, D.Z., et al., *Inorg. Chem.*, 2008, vol. 47, no. 19, p. 8748.
23. Feng, X., Feng, Y.Q., Liu, L., et al., *Dalton Trans.*, 2013, vol. 42, no. 21, p. 7741.